Quantifying the Manning's n roughness coefficient for riparian vegetation classes using the Specht vegetation classification scheme

Jay Kumar Singh Chauhan[1], Kirstie Fryirs[1] and Nuosha Zhang[1]

1 School of Natural Sciences, Macquarie University, North Ryde, NSW, 2109, Australia. Email: jay.kumarsinghchauhan@hdr.mq.edu.au

Key points

- This paper introduces a TLS + voxel-based method to empirically derive Manning's n, replacing subjective lookup tables with physically based, 3D vegetation measurements.
- Flow depth- and velocity-dependent roughness curves are developed for 10 Specht vegetation classes, showing Manning's n varies systematically with flow conditions and riparian vegetation type.
- The findings allow users to link roughness values to Specht vegetation classes, enabling standardised, field-applicable estimation using simple vegetation structural attributes (height, cover, form).
- The findings provide more accurate Manning's n numbers for parameterisation of hydraulic models, allowing more spatially variable roughness inputs at reach and corridor scales.
- The Specht-based Manning's n roughness numbers could be used to support the design of riparian revegetation programs and scenario modelling for effective NFM implementation.

Abstract

Over the past three decades, both the frequency and magnitude of floods have increased globally, with the 2021–2022 eastern Australian floods underscoring the vulnerability of conventional flood management approaches and the need for effective nature-based alternatives. Natural Flood Management (NFM) offers a sustainable framework for mitigating flood risk. The most common way that NFM is delivered on-the-ground is by increasing the vegetative roughness of river channels, riparian zones and catchments. However, the estimation of vegetation-induced hydraulic roughness, commonly represented by the Manning's roughness coefficient (n), is almost always reliant on visual guide, look-up tables and expert judgement, introducing substantial uncertainty into flood modelling. This study quantifies Manning's n values across the full spectrum of Specht vegetation classes, ranging from groundcover to rainforest. The Specht classification scheme is widely used in Australia for vegetation classification. Depth-dependent Manning's n curves are developed to capture how hydraulic roughness evolves with increasing flow depth and velocity across different vegetation classes.

The study advances the application of Terrestrial Laser Scanning (TLS) to estimate Manning's n through robust, voxel-based quantification of vegetation surface area. The resulting Manning's n values enhance the representation of riparian vegetation by explicitly accounting for structural attributes including vegetation height, growth form, and canopy cover. These findings offer transferable roughness estimates for riparian environments classified using the Specht system and provide improved parameterization for a wide range of applications, including NFM modelling and the design of on-ground river rehabilitation, riparian vegetation management and replanting programs.

Keywords

Natural Flood Management (NFM), Hydraulic roughness, River rehabilitation, Specht vegetation classification, Flood modelling, Geomorphic resilience

Introduction

Between 2021 and 2025, eastern New South Wales (NSW) experienced a series of extreme flood events driven by persistent La Niña phases and intensified rainfall associated with a warming climate (BoM, 2022). Major coastal catchments across the Northern Rivers, Sydney Basin, Hunter, and mid-north coast regions were repeatedly affected, with some floods ranking among the largest on record (BoM, 2023; Fryirs et al., 2023). The February–March 2022 Northern Rivers floods were particularly devastating, becoming one of the costliest natural disasters in Australian history, with insured losses exceeding AUD $6.4 billion (BoM, 2022; Insurance Council of Australia, 2023). Subsequent inquiries called for the implementation of nature-based flood mitigation, including large-scale revegetation and wetland restoration (O'Kane and Fuller, 2022), prompting increased interest in Natural Flood Management (NFM) as an approach to "slow and lower the flow" (Lane, 2017; Fryirs et al., 2023; Fryirs, 2026). A key component of NFM is riparian vegetation management to increase hydraulic roughness. However, current hydrodynamic models still rely on lookup tables for Manning's n and do not adequately represent the complexity of multi-layered vegetation (Chaulagain et al., 2022).

Manning's n is one of the most widely applied roughness coefficients in open-channel hydraulics (Chow, 1959; Arcement & Schneider, 1989; Wohl, 1998), yet its estimation remains highly dependent on expert judgement. Vegetation-induced roughness varies with plant form and structure, and while empirical models incorporating traits such as stem density, leaf area index, and morphology exist (Järvelä, 2004; Baptist et al., 2007; Jalonen et al., 2013; Li et al., 2015), they are sensitive to parameters such as drag coefficient and reconfiguration (Straatsma & Baptist, 2008; Wang & Zhang, 2019; Fathi-Moghadam et al., 2024). This study refines these formulations using updated vegetation-specific parameters (Box et al., 2024) and adopts the Specht vegetation classification to capture structural diversity across vegetation types (Specht, 1970; Thackway et al., 1995). Using Terrestrial Laser Scanning (TLS), high-resolution three-dimensional representations of vegetation are generated to estimate surface area, density, and porosity through voxel-based methods (Kukko et al., 2012; Dassot et al., 2011; Morsdorf et al., 2009; Jalonen et al., 2015; Straatsma et al., 2008). This enables more physically realistic parameterisation of resistance and improved estimation of Manning's n. The study aims to quantify Manning's n across a range of Specht vegetation classes, develop depth-dependent roughness curves, advance TLS-based approaches, and discuss the utility of having better estimates for NFM modelling and river rehabilitation design.

Study area and methods

This study focuses on the North Coast of New South Wales (NSW), Australia, specifically the Richmond River catchment and its sub-catchments, Terania Creek and Tuntable Creek, where extensive riparian replanting for Natural Flood Management (NFM) is currently underway after the 2022 floods (Figure 1). For this study, 10 classes of vegetation were selected from the Specht classification scheme (Specht, 1970) (Figure 2). The classes reflect the variety of vegetation characteristics most commonly found in natural channels, riparian zones and on floodplains. The 10 classes cover a spectrum ranging from grasslands to rainforest. The classes selected are as follows: Tall Closed Forest (TCf), Closed Forest (Cf), Open Forest (Of), Woodland (Wd), Low Closed Forest (LCf), Closed Scrub (Cs), Open Scrub (Os), Closed Tussock Grassland or Sedgeland (Cg), Dense Sown Pasture (Dp) and Sparse Open Herbfield (Sh).

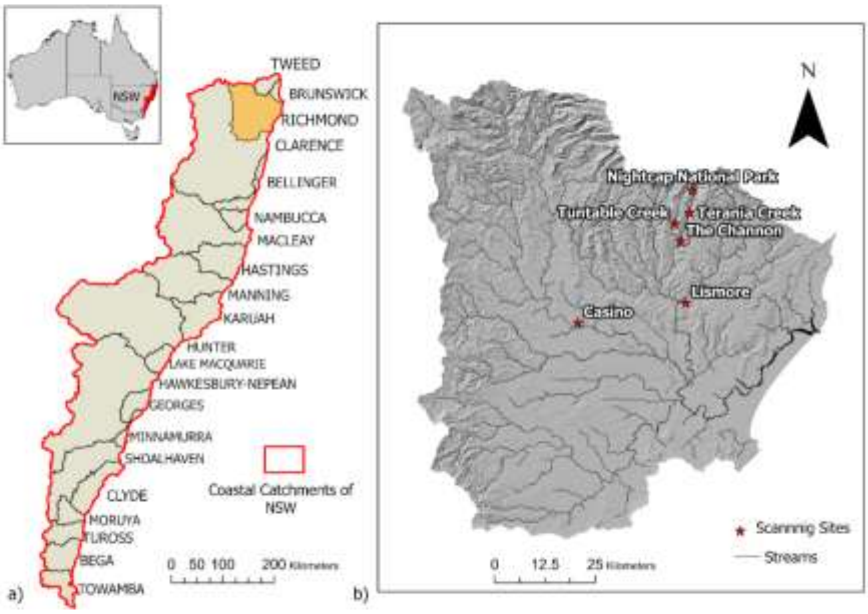

Figure 1 (a) Location of the Richmond catchment within coastal catchments of NSW, Australia (b) Vegetation scanning sites across the Richmond Catchment

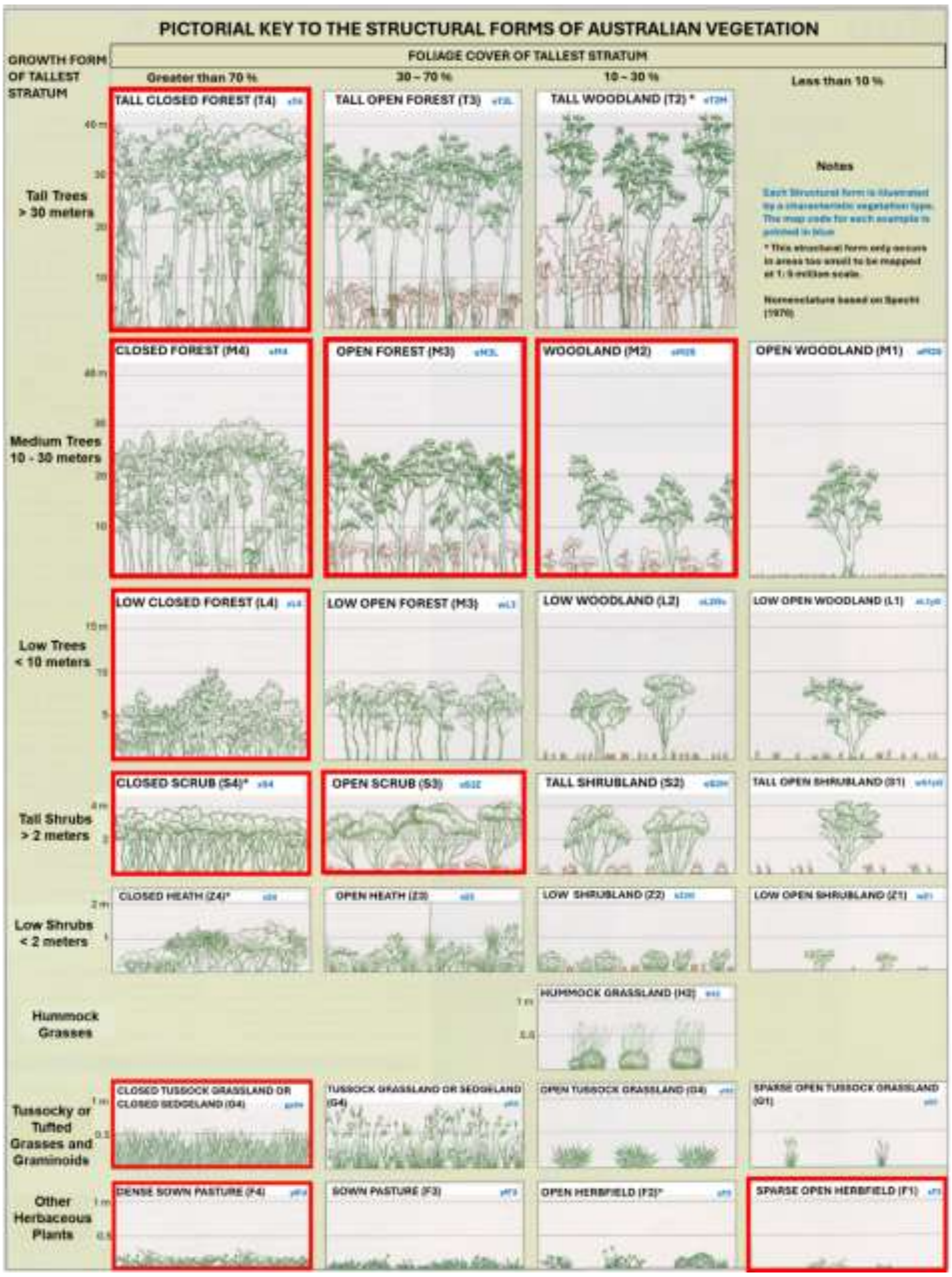

Figure 2 Specht vegetation classes selected for this study (Atlas of Australian Resources (1990), modified after Specht, 1970)

Terrestrial laser scanning

A total of 17 plots were scanned to capture structural variability across vegetation classes (workflow in Figure 3a), with most classes represented by two plots to allow replication. Each 30 × 30 m plot was subdivided into nine 10 × 10 m grids, with scans conducted at the center of each grid cell to minimise occlusion effects (Figure 3b). Scanning was performed using a RIEGL VZ-400 TLS, with a 0-360° horizontal and 30-130° vertical field of view, and a resolution of 0.06° in both directions. Fine scanning of 10cm cylindrical reflectors were used as tie points for registering the nine scans. The positions of the scanner and reflectors were surveyed using an Emlid Reach RS3 DGPS to ensure accurate georeferencing during post-processing.

Vegetation roughness estimation

We adopted two equations from Box et al. (2024) to calculate the Darcy-Weisbach friction factor f, for emergent H ≤ hc and submerged conditions H ≥ hc (where H is flow height, hc, is height of the vegetation) as follows (Equations 1 and 2):

$$f = \frac{8g}{\left[\left(\frac{1}{{C_b}^2} + \frac{C_{D\chi}\, PAI \left(\frac{U_c}{U_\chi}\right)^{\chi} \left(\frac{H}{h_c}\right)}{2g}\right)\right]} \quad , \; for\ H \leq h_c \qquad (1)$$

$$f = \frac{8g}{\left[\left(\frac{1}{{C_b}^2} + \frac{C_{D\chi}\, PAI \left(\frac{U_c}{U_\chi}\right)^{\chi}}{2g}\right)^{-0.5} + \frac{\sqrt{g}}{\alpha\kappa} \ln\left(\frac{H}{h_c}\right)\right]}, \quad for\ H \geq h_c \qquad (2)$$

Where $C_{D\chi}$ is the species-specific drag coefficient. The reconfiguration parameter χ, U_c, the flow velocity, and Uχ is the reference velocity used in determining $C_{D\chi}$. Other parameters in the models are Plant Area Index (PAI), C_b is Chezy's Bed coefficient, hc is the height of the vegetation, H is the flow height, κ is von Kármán constant, α is von Kármán scaling factor and gravitational acceleration g (= 9.81 ms^{-2}). Manning's n then can be derived from the Darcy-Weisbach friction factor (Equation 3).

$$n = {R_h}^{\frac{1}{6}} \sqrt{\frac{f}{8g}} \qquad (3)$$

The hydraulic radius, R_h, is equal to the cross-sectional area of flow divided by the wetted perimeter; therefore, in a wide floodplain the hydraulic radius is approximate to the depth of flow (Acrement and Schneider 1989).

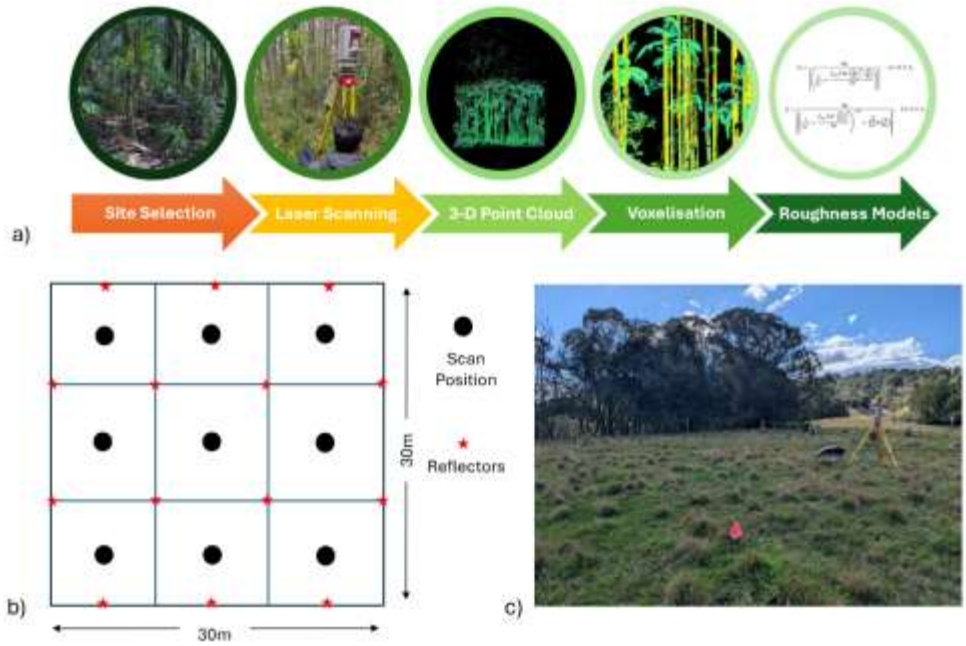

Figure 3 (a) Workflow and voxelisation of vegetation structure derived from terrestrial laser scanning. (b) Scanning protocol showing the arrangement of reflector targets and scanner positions and (c) field set-up of the Terrestrial Laser Scanner (TLS) during data acquisition

Results

Across the 10 vegetation classes and 17 plots, 153 individual scans were produced, yielding registered point clouds and voxelised outputs for each plot. An example is shown in Figure 4 for the Closed Forest (Cf) Specht vegetation class. The vertical surface area profiles reveal that structural complexity across most classes is concentrated within the 1 to 3 m understory zone, with the strongest contributions occurring in the Open Forest (Of), Low Closed Forest (LCf), and Open Scrub (Os) vegetation classes.

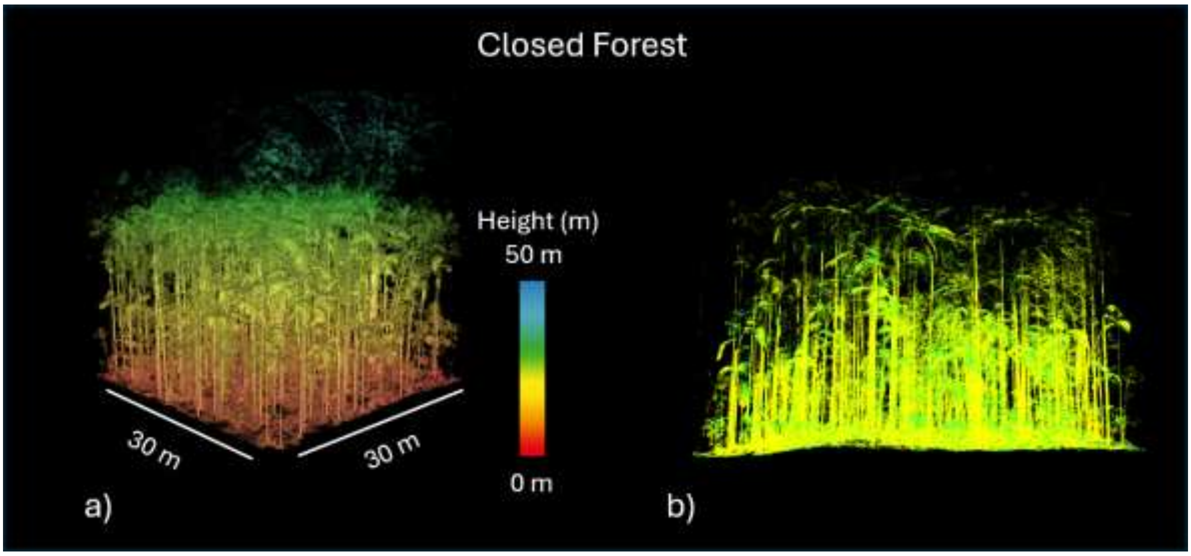

Figure 4 Example of a TLS scan for the Closed Forest (Cf) Specht vegetation class showing how the three Specht classification metrics have been captured; vegetation height, canopy cover percentage, and growth form. a) TLS Point cloud b) 3-D Voxel model of Closed forest

Manning's n varies systematically with vegetation structure and flow conditions, with clear separation between woody and non-woody vegetation classes (Figure 5). The results were generated for three velocity scenarios (0.5 ms^{-1}, 1 ms^{-1} and 2.5 ms^{-1}) which are commonly observed in overbank flood conditions (Arash et al., 2023). In general, n values decreased with increasing velocity across all vegetation classes, reflecting the inverse relationship between flow energy and hydraulic resistance (Box et al., 2022). At 0.5 ms^{-1}, woody vegetation classes produce substantially higher roughness values than non-woody classes across all flow depths, with Open Forest consistently producing the highest Manning's n of all classes across the full depth range, reflecting the progressive engagement of its dense flexible understory as flow depth increases. Manning's n decreases with increasing velocity across all classes, with the reduction ranging from approximately 31% for Sparse Open Herbfield (Sh) to 47% for Tall Closed Forest (TCf), Closed Forest (Cf), and Low Closed Forest (LCf), confirming the inverse relationship between flow energy and hydraulic resistance.

The depth-dependent behaviour of Manning's n differs systematically between vegetation classes (Figure 5). Woody vegetation classes display a continuous increase in Manning's n across the full measured depth range of 0.5 to 15 m, with no post-submergence decline, reflecting their tall multi-layered canopy structure. Tall Closed Forest (TCf) increases from 0.054 at 0.5 m depth to 0.189 at 15 m depth at 0.5 ms^{-1}, while Open Forest (Of) increases from 0.040 to 0.208 over the same range, the largest absolute increase of all classes. Closed Forest (Cf) follows a closely comparable trajectory (0.080 to 0.193 at 0.5 ms^{-1}), while Low Closed Forest (LCf) (0.051 to 0.185 at 0.5 ms^{-1}) and Woodland (Wd) (0.061 to 0.175 at 0.5 ms^{-1}) show similar depth-dependent increases with slightly flatter profiles above approximately 8 to 10 m as the upper canopy is progressively submerged.

Non-woody classes exhibit a distinct depth response governed by the height at which full canopy submergence occurs. Sparse Open Herbfield (Sh) reaches peak Manning's n at approximately 1 m depth (0.045 at 0.5 ms^{-1}) and remains essentially stable across the full depth range, as the sparse low-stature grass vegetation is submerged at very shallow depths. Dense Sown Pasture (Dp) peaks at approximately 2 m depth (0.084 at 0.5 ms^{-1}) before declining as the standing canopy is progressively submerged. Closed Tussock Grassland or Sedgeland (Cg) reaches peak resistance at approximately 8 m depth (0.090 at 0.5 ms^{-1}) before declining gradually, reflecting the taller and more rigid basal structure of tussock and sedge relative to pasture grasses. Closed Scrub (Cs) reaches peak Manning's n at approximately 9 m depth (0.150 at 0.5 ms^{-1}) before declining post-submergence, while Open Scrub (Os) peaks earlier at approximately 6.5 m depth (0.116 at 0.5 ms^{-1}), consistent with its lower and more open canopy structure.

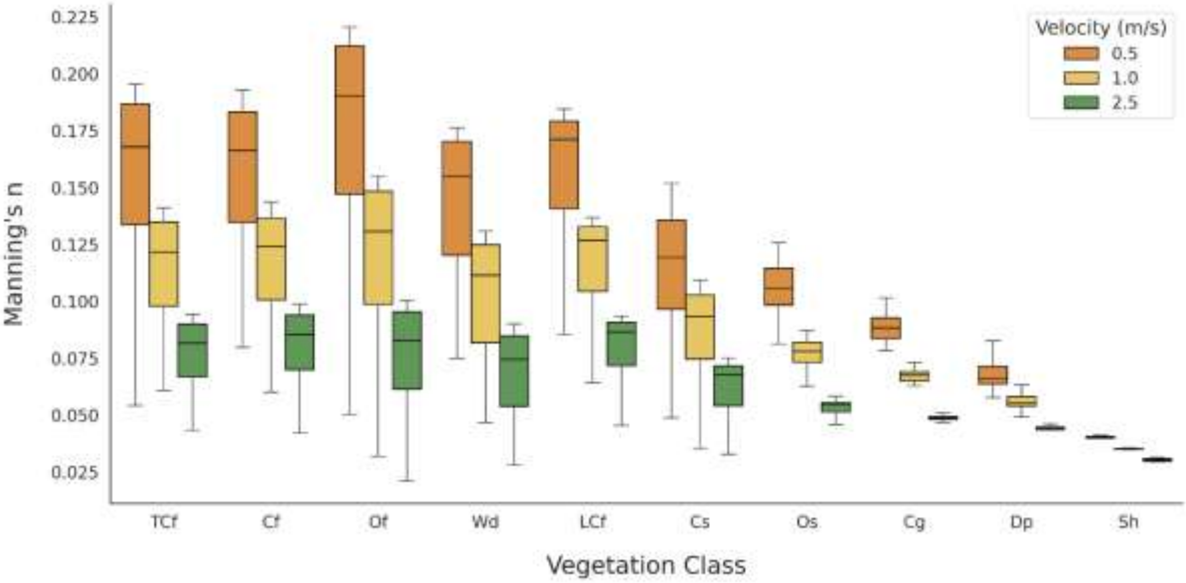

Figure 5 Manning's n for each of the 10 Specht vegetation classes (Chauhan et al., in Review). The x-axis shows the classes from left to right as per the Specht classification scheme with decreasing plant height and canopy cover. Tall Closed Forest (TCf), Closed Forest (Cf), Open Forest (Of), Woodland (Wd), Low Closed Forest (LCf), Closed Scrub (Cs), Open Scrub (Os), Closed Tussock Grassland or Sedgeland (Cg), Dense Sown Pasture (Dp) and Sparse Open Herbfield (Sh)

Variability in Manning's n also differs across vegetation types. Open Forest (Of) exhibits the widest range across the full depth-velocity envelope (0.025 at 0.5 m depth and 2.5 ms^{-1} to 0.208 at 15 m depth and 0.5 ms^{-1}), indicating strong sensitivity to both flow depth and velocity attributable to its flexible multi-layered understory. Sparse Open Herbfield (Sh) shows the narrowest range (0.024 to 0.045), consistent with its minimal and rapidly submerged vegetation structure.

A full practical reference guide for selecting depth-resolved values, presenting Manning's n at representative flow depth increments for 10 Specht vegetation classes is currently under development and review in Chauhan et al. (in review). The lead author can be contacted to confirm when these results have been finalised and are ready for use.

Discussion

Resolving uncertainty in Manning's n for riparian vegetation

Flood and hydrodynamic modelling have long relied upon tabulated Manning's n coefficients derived from expert judgment and photographic guides that are inherently subjective and prone to user bias (Chow, 1959; Arcement & Schneider, 1989).

Natural river channel and floodplain environments exhibit high spatial heterogeneity of vegetation (Box et al., 2024; Järvelä, 2004; Signorile et al., 2024; Straatsma et al., 2008). Uniform application of Manning's n across different vegetation classes and flow conditions oversimplifies this heterogeneity (Manners et al., 2013; Barinas et al., 2024). Although Manning's n is widely recognised to vary with vegetation type, density, and flow depth (Järvelä, 2004; Nepf, 2012), the absence of standardised quantification has led to uniform or average roughness values being routinely applied in hydraulic models (Shields et al., 2017; Wang & Zhang, 2019), compromising model accuracy and predictive reliability (Mason et al., 2003; Mewis, 2021). Existing literature reports n values ranging from 0.040 to 0.500 depending on vegetation and flow conditions (Chow, 1959; Kouwen & Fathi-Moghadam, 2000; Antonarakis et al., 2010), but generally lacks explicit consideration of flow depth, a critical gap this study addresses (Sharpe et al., 2023; Box et al., 2024; Barinas et al., 2024; Signorile et al., 2024).

The present study advances existing methods in two important respects. First, terrestrial laser scanning captures the full three-dimensional vegetation volume, including understory layers, that two-dimensional photographs and manual stem counts miss. By using refined equations from Box et al. (2024) this study has incorporated vegetation parameters that have been overlooked in earlier formulations, namely the reconfiguration parameter, species-specific drag coefficient, and reference velocity into the Manning's n coefficient quantification. Second, the Specht vegetation classification scheme provides a simple classification scheme that can be readily deployed in the field or using images. It is also not species specific because it focusses on vegetation structure. Three observable structural attributes, namely vegetation height, canopy cover percentage, and growth form, is all that is needed to assign a Specht vegetation class at a plot, a site or along a reach (Figure 6). When the full reference guide is completed and published (Chauhan et al., in review) a practitioner will simply need to know the Specht vegetation class and the flow depth being considered, and assign the corresponding Manning's n coefficient (Figure 6). There will be no need for practitioners to do TLS surveys or the computation of TLS scans. The This removes the expert-judgment step inherent in matching sites to coarse photographic guides and general vegetation descriptions. It replaces these methods with a consistent, instrument-free classification that is generic and can be applied across regions and climate settings. The roughness envelopes created in this study span flow depths from 0.5 m to 15 m across velocities typical of overbank flooding (0.5, 1.0, and 2.5 ms^{-1}) (Figure 4) meaning that a user can determine what flow or flood depth will be modelled and apply an accurate Manning's n coefficient.

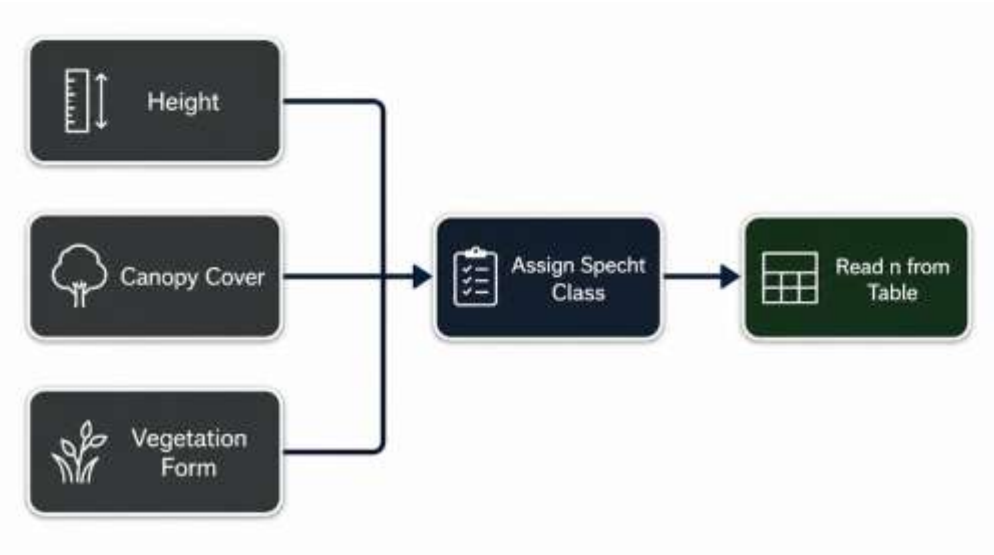

Figure 6 Workflow for using the Manning's n from the table

Potential future uses of the Specht vegetation classes Manning's n coefficient

The findings of this study have potential for transferability to any other riparian environments that can be classified using Specht vegetation classes. For example, a pine forest in the United States could be assigned to an open or closed forest class in the same way that riparian vegetation in eastern Australia is classified here. The Manning's n values generated enhance the resolution of vegetation representation by encompassing a broad spectrum of structural attributes, including height, form, and canopy cover (Chaulagain et al., 2022; Manners et al., 2013). The 10 vegetation classes selected, that range from grasses and shrubs to woodlands, open forests, and closed forests, capture the progression of structural complexity from herbaceous cover to rainforest conditions (Baker et al., 2020; Mewis, 2021). The depth-dependent roughness envelopes developed for a range of velocities provide a robust basis for calibrating hydraulic models, particularly two-dimensional flood models where spatial variability in roughness is critical (Barinas et al., 2024; Mason et al., 2003; Wang et al., 2019).

This classification framework could also be used to consider how hydraulic roughness evolves with vegetation maturity at-a-site or between-sites (Barinas et al., 2024; Mabbott et al., 2022). Linking roughness estimates to Specht vegetation classes establishes a scalable framework for parameterisation using remote sensing or vegetation maps (Forzieri et al., 2012; Forzieri et al., 2011). This could be used to run scenarios that facilitate catchment-scale implementation of nature-based solutions, determining where vegetation structure can be strategically managed to achieve desired hydraulic outcomes (Shields et al., 2017; Thomas et al., 2007). Such utility can dramatically improve the ability to determine where increased vegetative roughness could have best effect to attenuate flood peaks and deliver Natural Flood Management (NFM) (Lane, 2017; Fryirs 2026). Degraded catchments, for example, could benefit from targeted riparian revegetation programs aimed at regenerating or enhancing hydraulic roughness in priority zones (Krzeminska et al., 2019; Mabbott & Fryirs, 2022; Prinsley et al., 2025).

Beyond site-specific applications, this work supports the generation of roughness maps at larger spatial scales. By linking Manning's n values to Specht vegetation classes, the approach enables integration with remote sensing products and existing vegetation databases for catchment and region-scale quantification of riparian or terrestrial roughness (Forzieri et al., 2011; Prior et al., 2021). For instance, datasets such as those provided by Scarth et al. (2019), which offer 30-m spatial resolution maps of Australian forest and woodland structure (including height and canopy cover), could be used to extend roughness estimation across catchments or regions. This capability facilitates scalable implementation of river rehabilitation and NFM strategies and supports nature-based solutions for flood risk management by aligning vegetation structure with hydraulic performance objectives.

Conclusions

This study presents depth- and velocity-specific Manning's n roughness coefficients for ten riparian vegetation classes derived from Terrestrial Laser Scanning, expressed as continuous roughness envelopes spanning flow depths from 0.5 to 15 m across three flood velocities. By capturing the full three-dimensional vegetation structure, including understory layers that conventional two-dimensional survey methods routinely disregard, the TLS-derived values provide a more physically rigorous basis for hydraulic roughness parameterisation than existing visual lookup table approaches. Using the Specht structural classification scheme, based on three field-observable attributes of vegetation height, canopy cover, and growth form, enables practitioners to assign Manning's n values from field survey or satellite-derived vegetation maps without specialist instrumentation, removing the expert-judgment step inherent in existing photographic guides and supporting consistent application across regions and climate settings.

The results demonstrate that vegetation structure exerts a strong and systematic influence on hydraulic roughness that varies significantly with both flow depth and velocity. Structurally complex classes such as open forest and closed forest generate the highest roughness values, with open forest producing the greatest resistance at low velocities owing to its dense flexible understory, a contribution unresolved by prior references and of direct relevance to revegetation planning. These findings confirm that riparian revegetation programs targeting flood attenuation should prioritise structural complexity, canopy cover, and understory density, as sparse or low-stature vegetation classes generate comparatively low roughness at typical overbank depths. The Specht-class-linked roughness envelopes can be integrated with existing satellite-derived vegetation mapping products to produce spatially continuous Manning's n surfaces for one- and two-dimensional flood models, enabling catchment-scale scenario analysis of targeted revegetation, identification of priority zones for NFM intervention, and quantitative projection of how progressive revegetation toward structurally complex would attenuate flood peaks over time.

Acknowledgements

This work is funded by an Australian Research Council Linkage grant (LP230100011) to Macquarie University, with NSW Government partners Hunter Local Land Services (LLS), North Coast LLS, South-East LLS, and NSW Department of Climate Change, Energy, the Environment and Water – Surface Water Science Unit. We particularly thank Louissa Rogers at Richmond Landcare Inc. who arranged access to field sites and Joshua Cooper for field assistance. JC is supported by an International Macquarie Research Excellence Scholarship (iMQRES) & Macquarie University Higher Degree Research Funds. We acknowledge the Traditional Custodians of the land and rivers upon which this research reports and pay our respects to elders past and present.

References

Arcement, G., & Schneider, V. (1989). *Guide for selecting Manning's roughness coefficients for natural channels and flood plains* [Report](2339). (Water Supply Paper, Issue. G. P. O. U.S, B. For sale by the, & U. S. G. S. Open-File Reports Section. https://pubs.usgs.gov/publication/wsp2339

Atlas of Australian Resources - vol. 6, vegetation, AUSLIG, Canberra, 1990

Box, W., Järvelä, J., & Västilä, K. (2024). New formulas addressing flow resistance of floodplain vegetation from emergent to submerged conditions. *International Journal of River Basin Management*, *22*(3), 333-349. https://doi.org/10.1080/15715124.2022.2143512

Bureau of Meteorology. (2022). *New South Wales in 2022: Annual climate summary*. https://www.bom.gov.au/climate/current/annual/nsw/archive/2022.summary.shtml

Bureau of Meteorology. (2023). *Australia's climate and weather in 2023 summary graphic*. https://www.bom.gov.au/climate/current/annual/aus/2023/summary-graphic-2023.pdf

Chauhan, JKS., Fryirs, K., & Zhang, N. (2026). *Quantifying the Manning's n roughness coefficient across a gradient of riparian vegetation classes using Terrestrial Laser Scanning (TLS)*. *In review*.

Chaulagain, S., Stone, M. C., Dombroski, D., Gillihan, T., Chen, L., & Zhang, S. (2022). An investigation into remote sensing techniques and field observations to model hydraulic roughness from riparian vegetation. *River Research and Applications*, *38*(10), 1730-1745. https://doi.org/https://doi.org/10.1002/rra.4053

Fathi-Moghadam, M., Salmanzadeh, S., Ahadiyan, J., & Sajadi, M. (2024). Drag Coefficient of Rigid and Flexible Deciduous Trees in Riparian Forests. *Journal of Hydraulic Engineering*, *150*(5), 04024027. https://doi.org/doi:10.1061/JHEND8.HYENG-13709

Flynn, W. R. M., Owen, H. J. F., Grieve, S. W. D., & Lines, E. R. (2023). Quantifying vegetation indices using terrestrial laser scanning: methodological complexities and ecological insights from a Mediterranean forest. *Biogeosciences*, 20(13), 2769-2784. https://doi.org/10.5194/bg-20-2769-2023

Fryirs, K. (2026). Making sense of nature-based flood mitigation: A levers framework for conceptualising and communicating Natural Flood Management (NFM). *BioScience*. https://doi.org/10.1093/biosci/biag094

Fryirs, K., Zhang, N., Ralph, T. J., & Arash, A. M. (2023). Natural flood management: Lessons and opportunities from the catastrophic 2021–2022 floods in eastern Australia. *Earth Surface Processes and Landforms*, *48*(9), 1649-1664. https://doi.org/https://doi.org/10.1002/esp.5647

Jalonen, J., Järvelä, J., Virtanen, J.-P., Vaaja, M., Kurkela, M., & Hyyppä, H. (2015). Determining Characteristic Vegetation Areas by Terrestrial Laser Scanning for Floodplain Flow Modeling. *Water*, *7*(2), 420-437. https://www.mdpi.com/2073-4441/7/2/420

Järvelä, J. (2002). Flow resistance of flexible and stiff vegetation: a flume study with natural plants. *Journal of Hydrology*, *269*(1), 44-54. https://doi.org/https://doi.org/10.1016/S0022-1694(02)00193-2

Krzeminska, D., Kerkhof, T., Skaalsveen, K., & Stolte, J. (2019). Effect of riparian vegetation on stream bank stability in small agricultural catchments. *CATENA*, *172*, 87-96. https://doi.org/https://doi.org/10.1016/j.catena.2018.08.014

Mabbott, R., & Fryirs, K. (2022). Geomorphic and vegetative river recovery in a small coastal catchment of New South Wales, Australia: Implications for flow hydrology and river management. *Geomorphology*, *413*, 108334. https://doi.org/https://doi.org/10.1016/j.geomorph.2022.108334

Mewis, P. (2021). Estimation of Vegetation-Induced Flow Resistance for Hydraulic Computations Using Airborne Laser Scanning Data. *Water*, *13*(13), 1864. https://www.mdpi.com/2073-4441/13/13/1864

Prinsley, R., Sedighkia, M., Herath, P., Alexandra, J., Webster, T., Menzies, K., Croke, B., Hunt, S., Smith, J., Cordova, A., Falconer, N., Manning, M., & Wissing, K. (2025). *Nature-based Solutions for flood mitigation in Australia - Book 3: Practical Guide*. ANU Institute for Climate, Energy & Disaster Solutions. http://10.25911/E4YP-7G65

Signorile, A., Saracino, R., Dani, A., Rillo Migliorini Giovannini, M., & Preti, F. (2024). Riparian vegetation surveys for roughness estimation. *Ecological Engineering*, *209*, 107414. https://doi.org/https://doi.org/10.1016/j.ecoleng.2024.107414

Specht, R.L. Vegetation. In *Leeper, G.W. (ed.), "Australian Environment"*; Melbourne University Press: Melbourne, Australia, 1970; pp. 44–67.

Straatsma, M. W., & Baptist, M. J. (2008). Floodplain roughness parameterization using airborne laser scanning and spectral remote sensing. *Remote Sensing of Environment*, *112*(3), 1062-1080. https://doi.org/https://doi.org/10.1016/j.rse.2007.07.012

Scarth, P., Armston, J., Lucas, R., & Bunting, P. (2019). A Structural Classification of Australian Vegetation Using ICESat/GLAS, ALOS PALSAR, and Landsat Sensor Data. *Remote Sensing*, *11*(2), 147. https://www.mdpi.com/2072-4292/11/2/147